Supporting Information:

Understanding the Impact of Different Types of Surface States on Photoelectrochemical Water Oxidation: A Microkinetic Modeling Approach

Kiran George,[1] *Tigran Khachatrjan,*[2] *Matthijs van Berkel,*[3,4] *Vivek Sinha,*[1,5] *and Anja Bieberle-Hütter*[1,*]

[1] Dutch Institute for Fundamental Energy Research (DIFFER), Electrochemical Materials and Interfaces, PO Box 6336, 5600 HH Eindhoven, The Netherlands.

[2] Eindhoven University of Technology, Department of Applied Physics, PO Box 513, 5600 MB Eindhoven, The Netherlands

[3] Dutch Institute for Fundamental Energy Research (DIFFER), Energy Systems & Control, PO Box 6336, 5600 HH Eindhoven, The Netherlands

*Corresponding author email: a.bieberle@differ.nl

S1. Microkinetic model of OER

The oxygen evolution reaction under alkaline environment is given by

$$4OH^- + 4h^+ \rightarrow O_2 + 2H_2O \quad \text{(S.1)}$$

In this study, reactions in an alkaline environment are considered and the mechanism proposed by Hellman et al.[1] is chosen. This mechanism is based on the multistep OER mechanism proposed earlier by Rossmeisl et al.[2]

S1.1 Electrochemical mechanism of OER

The four-step OER in alkaline environment is given as

$$* + OH^- + h^+ \underset{K_{\mathrm{b1}}}{\overset{K_{\mathrm{f1}}}{\rightleftharpoons}} OH_{\mathrm{ad}} \quad \text{(S.2)}$$

$$OH_{\mathrm{ad}} + OH^- + h^+ \underset{K_{\mathrm{b2}}}{\overset{K_{\mathrm{f2}}}{\rightleftharpoons}} O_{\mathrm{ad}} + H_2O \quad \text{(S.3)}$$

$$O_{\mathrm{ad}} + OH^- + h^+ \underset{K_{\mathrm{b3}}}{\overset{K_{\mathrm{f3}}}{\rightleftharpoons}} OOH_{\mathrm{ad}} \quad \text{(S.4)}$$

$$OOH_{\mathrm{ad}} + OH^- + h^+ \underset{K_{\mathrm{b4}}}{\overset{K_{\mathrm{f4}}}{\rightleftharpoons}} O_{2,\mathrm{ad}} + H_2O \quad \text{(S.5)}$$

Here * represents an adsorption site and the subscript *ad* means that the species are adsorbed on the surface. Thus, OH_{ad}, O_{ad}, OOH_{ad}, and $O_{2,\mathrm{ad}}$ are the intermediate species adsorbed on the surface during the OER. The forward and backward reaction rates of these charge transfer reactions are represented by K_{fi} and K_{bi}, respectively, where i = 1 to 4. The calculation of these rate constants is described in the following sections. After adsorbed oxygen ($O_{2,\mathrm{ad}}$) is formed at the site, it desorbs ($O_{2,\mathrm{des}}$) from the surface at a rate of K_{f5} which is given by

$$O_{2,\mathrm{ad}} \overset{K_{\mathrm{f5}}}{\rightarrow} O_{2,\mathrm{des}} + * \quad \text{(S.6)}$$

This step does not involve charge transfer and, hence, the desorption rate K_{f5} is chosen as a constant.

S1.2 Charge transfer via valence band and conduction band

Rate constants for charge transfer via valence band and conduction band

For an ideal semiconductor, charge transfer can occur via the valence band (VB) and/or via the conduction band (CB). The forward and backward rate constants for charge transfer via VB, $K_{\mathrm{v_{fi}}}$ and $K_{\mathrm{v_{bi}}}$ can be calculated as[3]

$$K_{\mathrm{v_{fi}}} = \overline{kv_{\mathrm{fi}}} p_{\mathrm{s}} \tag{S.7}$$

$$K_{\mathrm{v_{bi}}} = \overline{kv_{\mathrm{bi}}} N_{\mathrm{v}} \tag{S.8}$$

$$\overline{kv_{fi}} = k_{\mathrm{v,max,f}} \exp\left[-\frac{\left(E_{\mathrm{v}} - E^{0}_{\mathrm{F,redox,i}} - V_{\mathrm{H}} - \lambda\right)^2}{4\lambda K_{\mathrm{B}} T} \right] \tag{S.9}$$

$$\overline{kv_{bi}} = k_{\mathrm{v,max,b}} \exp\left[-\frac{\left(E_{\mathrm{v}} - E^{0}_{\mathrm{F,redox,i}} - V_{\mathrm{H}} + \lambda\right)^2}{4\lambda K_{B} T} \right] \tag{S.10}$$

where p_{s} is the hole density at the surface, N_{v} is the density of states of the valence band, E_{v} is the valence band energy level, $E_{\mathrm{redox,i}}$ is the redox potential of the intermediate steps (i = 1 to 4), V_{H} is the potential drop across the Helmholtz layer, λ is the solvent reorganization energy, k_{B} is the Boltzmann constant, and T is the temperature. The descriptions of all the parameters used in the model and their respective values are given in Table S1.

Table S1 Model parameters specific to the microkinetic model, their descriptions, and values in addition to Table 1 in the main manuscript.

Parameter	Description	Value	Ref.
K_{B}	Boltzmann constant	8.61733 x 10^{-5} eV/K	
e	Charge of electron	1.60217662 x 10^{-19} C	
ϵ_0	Permittivity of free space	8.8541878128 x 10^{-14} F cm^{-1}	
Sr	Scan rate	20 mV/s	
T	Temperature	298 K	

pH	pH of the electrolyte	13.6	
pOH	pOH of the electrolyte	14-pH	
x_{OH}	Mole fraction of hydroxyl ions	$10^{-\mathrm{pOH}}$/(molar conc. of water)	
x_{H2O}	Mole fraction of water	1-x_{OH}	
$k_{\mathrm{v,max,f}}$, $k_{\mathrm{v,max,b}}$	Max. rate constants via val. band	3 x 10^{-16} cm^4/s	4
$k_{\mathrm{c,max,f}}$, $k_{\mathrm{c,max,b}}$	Max. rate constants via cond. band	3 x 10^{-16} cm^4/s	4
$k_{\mathrm{t,max,f}}$, $k_{\mathrm{t,max,b}}$	Max. rate constants via trap state	3 x 10^{-16} cm^4/s	4
λ	Solvent reorganization energy	1 eV	5
N_{C}	Density of state of cond. band	4 x 10^{22} cm^{-3}	6
N_{V}	Density of state of val. band	1 x 10^{22} cm^{-3}	6
K_{f5}	Desorption rate of oxygen	8 x 10^5 cm^{-1}	7

Similarly, the rate constants for charge transfer via CB (subscript c) can be calculated as [3]

$$K_{\mathrm{c_{fi}}} = \overline{kc_{\mathrm{fi}}} N_{\mathrm{c}} \tag{S.11}$$

$$K_{c_{\mathrm{bi}}} = \overline{kc_{\mathrm{bi}}} n_{\mathrm{s}} \tag{S.12}$$

$$\overline{kc_{\mathrm{fi}}} = k_{\mathrm{c,max,f}}\, exp\left[-\frac{\left(E_{\mathrm{c}} - E^{0}_{\mathrm{F,redox,i}} - V_{\mathrm{H}} - \lambda\right)^2}{4\lambda K_{\mathrm{B}} T} \right] \tag{S.13}$$

$$\overline{kc_{bi}} = k_{\mathrm{c,max,b}}\, exp\left[-\frac{\left(E_{c} - E^{0}_{\mathrm{F,redox,i}} - V_{\mathrm{H}} + \lambda\right)^2}{4\lambda K_{\mathrm{B}} T} \right] \tag{S.14}$$

where N_{c} is the density of states of the conduction band, n_{s} is the electron density at the surface, and E_{c} is the conduction band energy level.

Rate equations for OER intermediates at semiconductor sites

The rate equations for fractional coverage of intermediates at a semiconductor site due to charge transfer via both VB and CB can be written as

$$\dot{\theta}_{\mathrm{OH}} = K_{\mathrm{vf1}} x_{\mathrm{OH}}\, \theta_{\mathrm{ad}} - K_{\mathrm{vb1}} \theta_{\mathrm{OH}} - K_{\mathrm{vf2}} \theta_{\mathrm{OH}} x_{\mathrm{OH}} + K_{\mathrm{vb2}} \theta_{\mathrm{O}} x_{\mathrm{H_2O}} + K_{\mathrm{cf1}} x_{\mathrm{OH}}\, \theta_{\mathrm{ad}} - K_{\mathrm{cb1}} \theta_{\mathrm{OH}} - K_{\mathrm{cf2}} \theta_{\mathrm{OH}} x_{\mathrm{OH}} + K_{\mathrm{cb2}} \theta_{\mathrm{O}} x_{\mathrm{H_2O}} \quad \text{(S.15)}$$

$$\dot{\theta}_{\mathrm{O}} = K_{\mathrm{vf2}} x_{\mathrm{OH}}\ \theta_{\mathrm{OH}} - K_{\mathrm{vb2}} \theta_{\mathrm{O}} x_{\mathrm{H_2O}} - K_{\mathrm{vf3}} \theta_{\mathrm{O}} x_{\mathrm{OH}} + K_{\mathrm{v}b3} \theta_{\mathrm{OOH}} + K_{\mathrm{cf2}} x_{\mathrm{OH}}\ \theta_{\mathrm{OH}} - K_{\mathrm{cb2}} \theta_{\mathrm{O}} x_{\mathrm{H_2O}} - K_{\mathrm{cf3}} \theta_{\mathrm{O}} x_{\mathrm{OH}} + K_{\mathrm{cb3}} \theta_{\mathrm{OOH}} \quad \text{(S.16)}$$

$$\dot{\theta}_{\mathrm{OOH}} = K_{\mathrm{vf3}} \theta_{\mathrm{O}} x_{\mathrm{OH}} - K_{\mathrm{v}b3} \theta_{\mathrm{OOH}} - K_{\mathrm{v}_f4} \theta_{\mathrm{OOH}} x_{\mathrm{OH}} + K_{\mathrm{vb4}} \theta_{\mathrm{O_2}} x_{\mathrm{H_2O}} + K_{\mathrm{cf3}} \theta_{\mathrm{O}} x_{\mathrm{OH}} - K_{\mathrm{cb3}} \theta_{\mathrm{OOH}} - K_{\mathrm{cf4}} \theta_{\mathrm{OOH}} x_{\mathrm{OH}} + K_{\mathrm{cb4}} \theta_{\mathrm{O_2}} x_{\mathrm{H_2O}} \quad \text{(S.17)}$$

$$\dot{\theta}_{\mathrm{O_2}} = K_{\mathrm{vf4}} \theta_{\mathrm{OOH}} x_{\mathrm{OH}} - K_{\mathrm{vb4}} \theta_{\mathrm{O_2}} x_{\mathrm{H_2O}} + K_{\mathrm{cf4}} \theta_{\mathrm{OOH}} x_{\mathrm{OH}} - K_{\mathrm{cb4}} \theta_{\mathrm{O_2}} x_{\mathrm{H_2O}} - K_{\mathrm{f5}} \theta_{\mathrm{O_2}} \quad \text{(S.18)}$$

$$\theta_{ad} = 1 - \theta_{\mathrm{OH}} - \theta_{O} - \theta_{OOH} - \theta_{O_2} \quad \text{(S.19)}$$

where x_{OH} represents the mole fraction of hydroxyl ions and $x_{\mathrm{H_2O}}$ represents the mole fraction of water.

Current density due to charge transfer via VB and CB

The forward and backward current densities for charge transfer via VB (subscript $_{\mathrm{V}}$) and CB (subscript $_{\mathrm{C}}$) are calculated as

$$j_{\mathrm{vf}} = eN_0\left(K_{\mathrm{vf1}} \theta_{\mathrm{ad}} + K_{\mathrm{vf2}} \theta_{\mathrm{OH}} + K_{\mathrm{vf3}} \theta_{\mathrm{O}} + K_{\mathrm{vf4}} \theta_{\mathrm{OOH}}\right) x_{OH} \quad \text{(S.20)}$$

$$j_{\mathrm{vb}} = eN_0\left(K_{\mathrm{vb1}} \theta_{\mathrm{OH}} + K_{\mathrm{vb2}} \theta_{\mathrm{O}} x_{\mathrm{H_2O}} + K_{\mathrm{vb3}} \theta_{\mathrm{OOH}} + K_{\mathrm{vb4}} \theta_{\mathrm{O_2}} x_{\mathrm{H_2O}}\right) \quad \text{(S.21)}$$

$$j_{\mathrm{v}} = j_{\mathrm{vf}} - j_{\mathrm{vb}} \quad \text{(S.22)}$$

$$j_{\mathrm{cf}} = eN_0\left(K_{\mathrm{cf1}} \theta_{\mathrm{ad}} + K_{\mathrm{cf2}} \theta_{\mathrm{OH}} + K_{\mathrm{cf3}} \theta_{\mathrm{O}} + K_{\mathrm{cf4}} \theta_{\mathrm{OOH}}\right) x_{\mathrm{OH}} \quad \text{(S.23)}$$

$$j_{\mathrm{c}b} = eN_0\left(K_{\mathrm{cb1}} \theta_{\mathrm{OH}} + K_{\mathrm{cb2}} \theta_{\mathrm{O}} x_{\mathrm{H_2O}} + K_{\mathrm{cb3}} \theta_{\mathrm{OOH}} + K_{\mathrm{cb4}} \theta_{\mathrm{O_2}} x_{\mathrm{H_2O}}\right) \quad \text{(S.24)}$$

$$j_{\mathrm{c}} = j_{\mathrm{cf}} - j_{\mathrm{cb}} \quad \text{(S.25)}$$

S1.3 Charge transfer via r-SS

Rate constants for charge transfer via r-SS

The surface states which act as recombination centers are called recombining surface states (r-SS). The rate constants for charge transfer via r-SS are calculated as [3]

$$K_{\mathrm{tfi}} = \overline{kt_{\mathrm{fi}}}(1 - f)(N_{\mathrm{T}}/d) \quad \text{(S.26)}$$

$$K_{t_{\mathrm{bi}}} = \overline{kt_{\mathrm{bi}}} f(N_{\mathrm{T}}/d) \tag{S.27}$$

$$\overline{kt_{\mathrm{fi}}} = k_{\mathrm{t,max,f}} \exp\left[-\frac{\left(E_{\mathrm{T}} - E^{0}_{\mathrm{F,redox,i}} - V_{\mathrm{H}} - \lambda\right)^2}{4\lambda K_{\mathrm{B}} T}\right] \tag{S.28}$$

$$\overline{kt_{\mathrm{bi}}} = k_{\mathrm{t,max,b}} \exp\left[-\frac{\left(E_{\mathrm{T}} - E^{0}_{\mathrm{F,redox,i}} - V_{\mathrm{H}} + \lambda\right)^2}{4\lambda K_{\mathrm{B}} T}\right] \tag{S.29}$$

where N_{T} is the density of states of r-SS, f is the fill factor of r-SS, d is the thickness of the hole accumulation layer, and is used to convert the surface concentration (per cm^2) to volume concentration (per cm^3).[8]

Rate equations for OER intermediates at sites corresponding to r-SS

The rate equations for fractional coverage of intermediates at an r-SS site due to charge transfer via r-SS are calculated as

$$\dot{\theta}T_{\mathrm{OH}} = K_{\mathrm{t_{f1}}} x_{\mathrm{OH}}\, \theta T_{\mathrm{ad}} - K_{\mathrm{t_{b1}}} \theta T_{\mathrm{OH}} - K_{\mathrm{t_{f2}}} \theta T_{\mathrm{OH}} x_{\mathrm{OH}} + K_{\mathrm{t_{b2}}} \theta T_{\mathrm{O}} x_{\mathrm{H_2O}} \tag{S.30}$$

$$\dot{\theta}T_{\mathrm{O}} = K_{\mathrm{t_{f2}}} x_{\mathrm{OH}}\, \theta T_{\mathrm{OH}} - K_{\mathrm{t_{b2}}} \theta T_{\mathrm{O}} x_{\mathrm{H_2O}} - K_{\mathrm{t_{f3}}} \theta T_{\mathrm{O}} x_{\mathrm{OH}} + K_{\mathrm{t_{b3}}} \theta T_{\mathrm{OOH}} \tag{S.31}$$

$$\dot{\theta T}_{\mathrm{OOH}} = K_{\mathrm{t_{f3}}} \theta T_{\mathrm{O}} x_{\mathrm{OH}} - K_{\mathrm{t_{b3}}} \theta T_{\mathrm{OOH}} - K_{\mathrm{t_{f4}}} \theta T_{\mathrm{OOH}} x_{\mathrm{OH}} + K_{\mathrm{t_{b4}}} \theta T_{\mathrm{O_2}} x_{\mathrm{H_2O}} \tag{S.32}$$

$$\dot{\theta T}_{\mathrm{O_2}} = K_{\mathrm{t_{f4}}} \theta T_{\mathrm{OOH}} x_{\mathrm{OH}} - K_{\mathrm{t_{b4}}} \theta T_{\mathrm{O_2}} x_{\mathrm{H_2O}} - K_{\mathrm{f5}} \theta T_{\mathrm{O_2}} \tag{S.33}$$

$$\theta T_{\mathrm{ad}} = 1 - \theta T_{\mathrm{OH}} - \theta T_{\mathrm{O}} - \theta T_{\mathrm{OOH}} - \theta T_{\mathrm{O_2}} \tag{S.34}$$

Current density due to charge transfer via r-SS

The forward and backward current densities for charge transfer via r-SS are calculated as

$$j_{\mathrm{t_f}} = eN_{\mathrm{ss}}\left(K_{\mathrm{t_{f1}}} \theta T_{\mathrm{ad}} + K_{\mathrm{t_{f2}}} \theta T_{OH} + K_{\mathrm{t_{f3}}} \theta T_{\mathrm{O}} + K_{\mathrm{t_{f4}}} \theta T_{\mathrm{OOH}}\right) x_{\mathrm{OH}} \tag{S.35}$$

$$j_{\mathrm{t_b}} = eN_{\mathrm{ss}}\left(K_{\mathrm{t_{b1}}} \theta T_{\mathrm{OH}} + K_{\mathrm{t_{b2}}} \theta T_{\mathrm{O}} x_{\mathrm{H_2O}} + K_{\mathrm{t_{b3}}} \theta T_{\mathrm{OOH}} + K_{\mathrm{t_{b4}}} \theta T_{\mathrm{O_2}} x_{\mathrm{H_2O}}\right) \tag{S.36}$$

$$j_{\mathrm{t}} = j_{\mathrm{t_f}} - j_{\mathrm{t_b}} \tag{S.37}$$

S1.4 Calculation of the total current density

The total current density is calculated based on Eq. S.20-S.25 and Eq. S.35-S.37 as

$$j = j_{\mathrm{v}} + j_{\mathrm{c}} + j_{\mathrm{t}} \tag{S.38}$$

$$j = j_{\mathrm{v_f}} + j_{\mathrm{c_f}} + j_{\mathrm{t_f}} - j_{\mathrm{v_b}} - j_{\mathrm{c_b}} - j_{\mathrm{t_b}} \tag{S.39}$$

S1.5 Implementation of IR drop in the model

The potential drop over the series resistance, R_s, depends on the current density in the circuit. The implementation of the potential drop over R_s in the model is shown as a schematic in Figure S1.

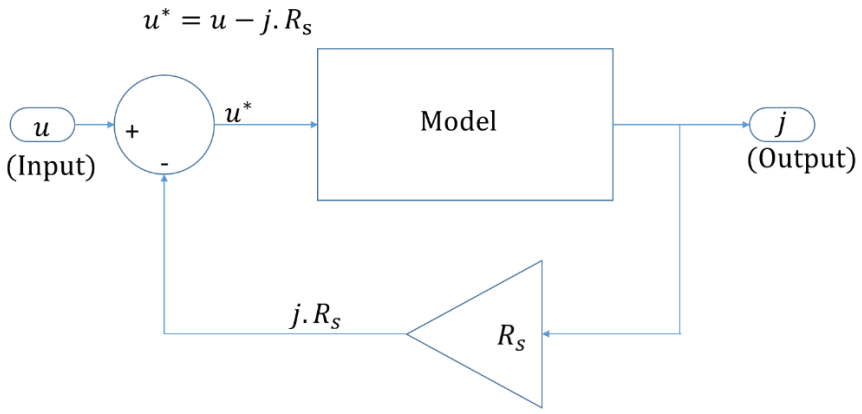

Figure S1 Schematic representation of the implementation of potential drop over the series resistance in the model; u^* represents the input potential to the model after correcting for a potential drop over R_s.

S2. Gibbs free energy and redox potential

The Gibbs free energies for the intermediates steps in OER on hematite are calculated using DFT.[9] Previously, in Zhang et al.[9], we have calculated Gibbs free energies for OER intermediates on hematite surfaces using DFT calculations, assuming a gas-solid interface. The gas-solid model does not account for solvent effects in the calculation of the free energies. In this study, an (implicit) solid-liquid model of the hematite-water interface is used wherein the solvent effects are accounted for by using a continuum solvation model with the dielectric constant of water (ϵ = 78.4) as implemented in VASPsol.[10] The redox potentials of the intermediate steps in OER are calculated using DFT. The spin-polarized DFT+U (U = 4.3 eV) formalism is chosen in order to treat the correlation effects in 3d electrons in hematite.[11] The Perdew–Burke–Ernzerhof (PBE) XC functional [12] and the projected augmented wave (PAW)[13] potentials were used. The molecular geometries were fully optimized with VASPsol when incorporating solvent effects. A 2x2 supercell of hematite (110) is used which is modeled as being antiferromagnetic (net zero spin via the MAGMOM keyword in VASP).[11,14] Zero-point energy correction and entropic contributions to the Gibbs free energy were obtained via Hessian calculation on the optimized geometry.

Table S2 Gibbs free energies calculated for OER intermediate steps on hematite (110) surface.

Parameter	Description	Value
ΔG_1	Gibbs free energy for the step in Eq. (S.2)	1.87 eV
ΔG_2	Gibbs free energy for the step in Eq. (S.3)	1.97 eV
ΔG_3	Gibbs free energy for the step in Eq. (S.4)	0.97 eV
ΔG_4	Gibbs free energy for the step in Eq. (S.5)	0.11 eV

The redox potential corresponding to each intermediate step can be calculated based on the relation between Gibbs free energy and redox potential given by[15]

$$E_{\text{redox,i}} = \frac{\Delta G_i}{nF} \tag{S.40}$$

where n is the number of electrons transferred in a single step (n = 1 for all steps here), F is the Faraday's constant, and $E_{\text{redox,i}}$ is the redox potential of the intermediate step.

S3. Experimental j-V plot for different illumination intensities

Experimental j-V plot for three different illumination intensities replotted from the literature for comparison with the simulations shown in Figure 3 of the main text.[16]

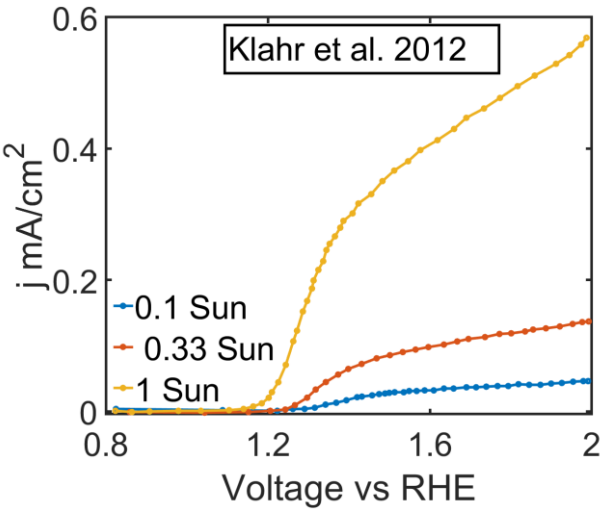

Figure S2 Experimental j-V plots for three different illumination intensities for hematite electrodes replotted from Klahr et al.[16]

S4. Simulated data for $R_s = 0$

The j-V curves, C_{i-SS} plots, and Mott-Schottky plots are simulated for three different illumination intensities by keeping $R_s = 0$ as shown in Figure S3. For all the three illumination intensities C_{i-SS} shows peaks around the OER onset potential. However, no deviation in linearity is observed in the Mott-Schottky plot around the potential range of C_{i-SS}. Therefore, the deviation in linearity observed in the Mott-Schottky plot in Figure 6 of the main text cannot be attributed to C_{i-SS}.

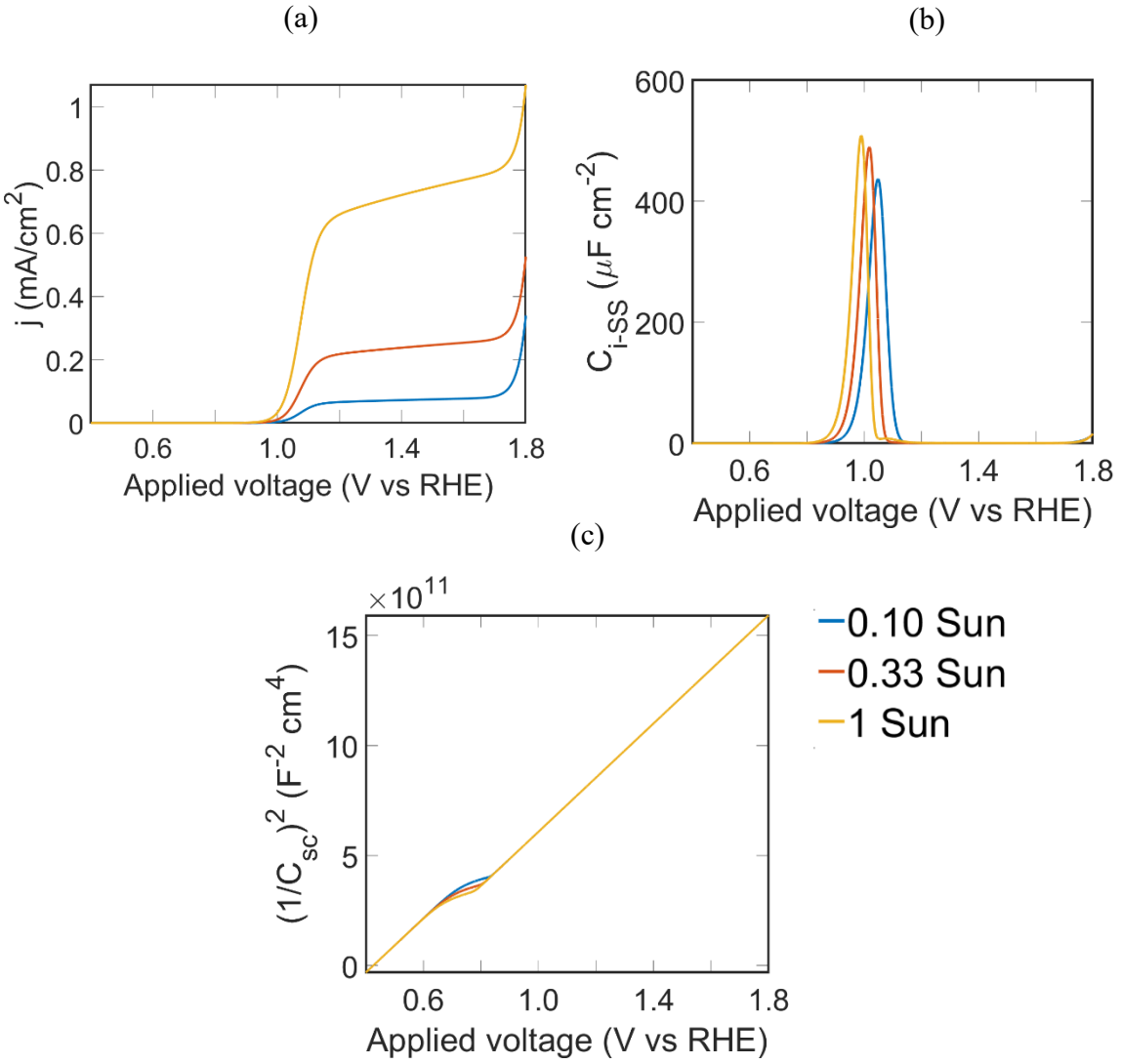

Figure S3 a) j-v plot, b) surface state capacitance C_{i-SS}, and c) Mott-Schottky plot simulated for the case of $R_s = 0$. The Mott-Schottky plot shows a deviation from linearity before the onset potential which is related to FLP due to r-SS. However, the Mott-Schottky plot shows no deviation in linearity around the potential range of C_{i-SS}.

S5. Coverage dependent Helmholtz capacitance

In the analysis of PEC data, the Helmholtz capacitance is usually assumed to be constant.[16,17] However, it has been reported in the literature that surface adsorption can affect the Helmholtz capacitance.[18] This will result in Helmholtz capacitance (C_{H}) to be potential dependent through the potential dependence of surface coverage. In this section, we look into a scenario in which the Helmholtz capacitance depends on the coverage of surface intermediates and how it affects the PEC data. For simulating the coverage-dependent Helmholtz capacitance, we consider the simplest model of Helmholtz capacitance which is based on a parallel plate capacitor.

The Helmholtz capacitance per unit area (C_{H0}) in this case, is defined as $C_{\mathrm{H0}} = \epsilon * \epsilon_0 / l$, where l is the thickness of the Helmholtz double-layer, ϵ_0 is the permittivity of free space, and ϵ is the relative permittivity of the semiconductor material.[19,20] An approximate value of 100 μF cm^{-2} is obtained for C_{H0} using $l = 3 \cdot 10^{-8}$ cm and $\epsilon = 38$[21] for hematite.

If we assume that the available area of the capacitor reduces due to surface adsorption, the capacitance based on potential can be calculated as $C_{\mathrm{H}} = C_{\mathrm{H0}} * \theta$, where θ is the fraction of free sites on the surface per unit area. We note that this is a simplified assumption. The idea here is to investigate whether a variation in Helmholtz capacitance based on surface coverage will affect the simulated data. Based on this assumption, the j-V plots, $C_{\mathrm{i-SS}}$, and Mott-Schottky plots are simulated for three different illumination intensities as shown in Figure S4. In these simulations, the contribution due to series resistance is eliminated by keeping $R_{\mathrm{s}} = 0$. Figure S4a shows the j-V plots for three different illumination intensities. $C_{\mathrm{i-SS}}$ plots from Figure S4b show peaks around respective OER onset potential. From Figure S4c, there are two points at which the Mott-Schottky plots show a deviation from linearity. The first one at lower potential is due to r-SS as described in the main text. The second deviation from linearity around the onset potential is enlarged and shown in Figure S4d. The potential range of this second deviation coincides with that of the peaks in the $C_{\mathrm{i-SS}}$ plot. In the main text, it is shown that potential drop over R_{s} can lead to a deviation in the Mott-Schottky plot around the onset potential. However, in this case $R_{\mathrm{s}} = 0$ and, hence, the deviation from linearity observed in the Mott-Schottky plot around the onset potential can be attributed to i-SS. Therefore, if the Helmholtz capacitance varies as a function of surface coverage, i-SS can result in FLP.

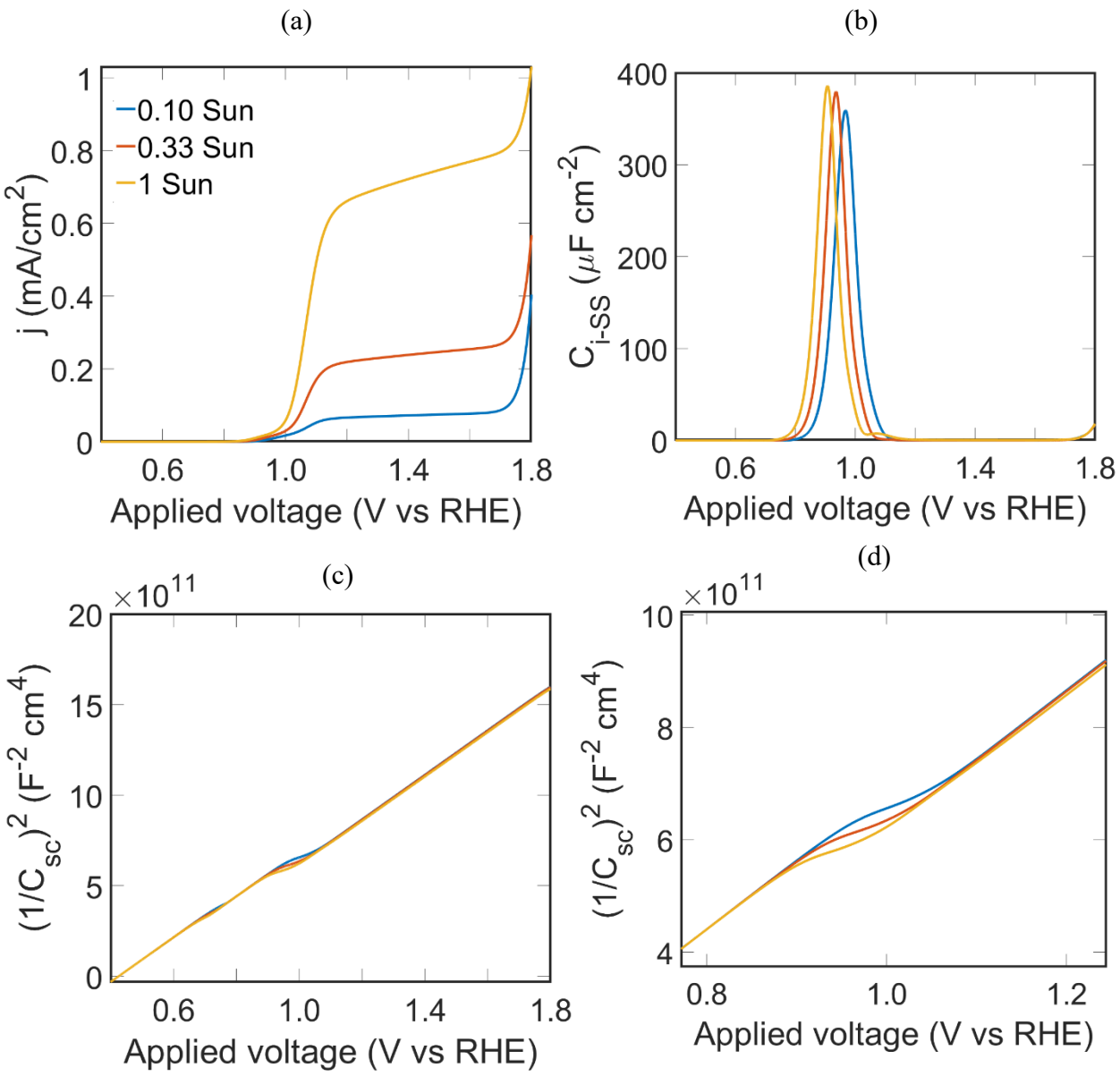

Figure S4 a) j-v plot, b) surface state capacitance $C_{\mathrm{i-SS}}$, c) Mott-Schottky plot simulated for the case of C_H varying as a function of surface coverage. R_s = 0 in all the simulations; d) Enlarged Mott-Schottky plot showing deviation in linearity around the onset potential when the Helmholtz potential is assumed to change with surface coverage, even when R_s = 0.

AUTHOR INFORMATION

[4] Eindhoven University of Technology, Mechanical Engineering, Control Systems Technology, PO Box 513, 5600 MB Eindhoven, The Netherlands.

[5] Delft University of Technology, Process and Energy Department, Faculty of Mechanical, Maritime and Materials Engineering, Leeghwaterstraat 39, 2628CB, Delft, The Netherlands.

References

(1) Hellman, A.; Iandolo, B.; Wickman, B.; Grönbeck, H.; Baltrusaitis, J. Electro-Oxidation of Water on Hematite: Effects of Surface Termination and Oxygen Vacancies Investigated by First-Principles. *Surf. Sci.* **2015**, *640*, 45–49.

(2) Rossmeisl, J.; Qu, Z. W.; Zhu, H.; Kroes, G. J.; Nørskov, J. K. Electrolysis of Water on Oxide Surfaces. *J. Electroanal. Chem.* **2007**, *607*, 83–89.

(3) Rüdiger, M. Charge Transfer Processes at the Semiconductor–Liquid Interface. In *Semiconductor Electrochemistry*; Wiley-Blackwell, 2015; pp 169–266.

(4) Lewis, N. S. Progress in Understanding Electron-Transfer Reactions at Semiconductor/Liquid Interfaces. *J. Phys. Chem. B* **1998**, *102*, 4843–4855.

(5) Heidaripour, A.; Ajami, N.; Miandari, S. Research of Gerischer Model in Transferring Electrons between Energy States of CdS Thin Film and Ferro-Ferric Redox System. **2015**, *3*, 59–64.

(6) Cendula, P.; David Tilley, S.; Gimenez, S.; Bisquert, J.; Schmid, M.; Grätzel, M.; Schumacher, J. O. Calculation of the Energy Band Diagram of a Photoelectrochemical Water Splitting Cell. *J. Phys. Chem. C* **2014**, *118*, 29599–29607.

(7) Hansen, H. A.; Viswanathan, V.; Nørskov, J. K. Unifying Kinetic and Thermodynamic Analysis of 2 e $^-$ and 4 e $^-$ Reduction of Oxygen on Metal Surfaces. *J. Phys. Chem. C* **2014**, *118*, 6706–6718.

(8) Peter, L. M. Energetics and Kinetics of Light-Driven Oxygen Evolution at Semiconductor Electrodes: The Example of Hematite. *J. Solid State Electrochem.* **2013**, *17*, 315–326.

(9) Zhang, X.; Klaver, P.; Van Santen, R.; Van De Sanden, M. C. M.; Bieberle-Hütter, A. Oxygen Evolution at Hematite Surfaces: The Impact of Structure and Oxygen Vacancies on Lowering the Overpotential. *J. Phys. Chem. C* **2016**, *120*, 18201–18208.

(10) http://vaspsol.mse.ufl.edu/.

(11) Liao, P.; Keith, J. A.; Carter, E. A. Water Oxidation on Pure and Doped Hematite (0001) Surfaces: Prediction of Co and Ni as Effective Dopants for Electrocatalysis. *J. Am. Chem. Soc.* **2012**, *134*, 13296–13309.

(12) Perdew, J. P.; Burke, K.; Ernzerhof, M. Generalized Gradient Approximation Made Simple. *Phys. Rev. Lett.* **1996**, *77*, 3865–3868.

(13) Blöchl, P. E. Projector Augmented-Wave Method. *Phys. Rev. B* **1994**, *50*, 17953–17979.

(14) Wang, R. B.; Hellman, A. Hybrid Functional Study of the Electro-Oxidation of Water on Pristine and Defective Hematite (0001). *J. Phys. Chem. C* **2019**, *123*, 2820–2827.

(15) George, K.; van Berkel, M.; Zhang, X.; Sinha, R.; Bieberle-Hütter, A. Impedance Spectra and Surface Coverages Simulated Directly from the Electrochemical Reaction Mechanism: A Nonlinear State-Space Approach. *J. Phys. Chem. C* **2019**, *123*, 9981–9992.

(16) Klahr, B.; Gimenez, S.; Fabregat-Santiago, F.; Hamann, T.; Bisquert, J. Water Oxidation at Hematite Photoelectrodes: The Role of Surface States. *J. Am. Chem. Soc.* **2012**, *134*, 4294–4302.

(17) van de Krol, R.; Grätzel, M. *Photoelectrochemical Hydrogen Production*; Springer: New York, 2012.

(18) Bohra, D.; Chaudhry, J. H.; Burdyny, T.; Pidko, E. A.; Smith, W. A. Modeling the Electrical Double Layer to Understand the Reaction Environment in a CO2 Electrocatalytic System. *Energy Environ. Sci.* **2019**, *12*, 3380–3389.

(19) Bard, A. J.; Bocarsly, A. B.; Fan, F. R. F.; Walton, E. G.; Wrighton, M. S. The Concept of Fermi Level Pinning at Semiconductor/Liquid Junctions. Consequences for Energy Conversion Efficiency and Selection of Useful Solution Redox Couples in Solar Devices. *J. Am. Chem. Soc.* **1980**, *102*, 3671–3677.

(20) Gongadze, E.; Petersen, S.; Beck, U.; Rienen, U. Van. Classical Models of the Interface between an Electrode and an Electrolyte. *Proc. COMSOL Conf. Milan* **2009**, 18–24.

(21) Shavorskiy, A.; Ye, X.; Karslloğlu, O.; Poletayev, A. D.; Hartl, M.; Zegkinoglou, I.; Trotochaud, L.; Nemšák, S.; Schneider, C. M.; Crumlin, E. J.; Axnanda, S.; Liu, Z.; Ross, P. N.; Chueh, W.; Bluhm, H. Direct Mapping of Band Positions in Doped and Undoped Hematite during Photoelectrochemical Water Splitting. *J. Phys. Chem. Lett.* **2017**, *8*, 5579–5586.